



OPEN

# Sofosbuvir terminated RNA is more resistant to SARS-CoV-2 proofreader than RNA terminated by Remdesivir

Steffen Jockusch<sup>1,4,5</sup>, Chuanjuan Tao<sup>1,2,5</sup>, Xiaoxu Li<sup>1,2</sup>, Minchen Chien<sup>1,2</sup>, Shiv Kumar<sup>1,2</sup>, Irina Morozova<sup>1,2</sup>, Sergey Kalachikov<sup>1,2</sup>, James J. Russo<sup>1,2</sup> & Jingyue Ju<sup>1,2,3</sup>✉

SARS-CoV-2 is responsible for COVID-19, resulting in the largest pandemic in over a hundred years. After examining the molecular structures and activities of hepatitis C viral inhibitors and comparing hepatitis C virus and coronavirus replication, we previously postulated that the FDA-approved hepatitis C drug EPCLUSA (Sofosbuvir/Velpatasvir) might inhibit SARS-CoV-2. We subsequently demonstrated that Sofosbuvir triphosphate is incorporated by the relatively low fidelity SARS-CoV and SARS-CoV-2 RNA-dependent RNA polymerases (RdRps), serving as an immediate polymerase reaction terminator, but not by a host-like high fidelity DNA polymerase. Other investigators have since demonstrated the ability of Sofosbuvir to inhibit SARS-CoV-2 replication in lung and brain cells; additionally, COVID-19 clinical trials with EPCLUSA and with Sofosbuvir plus Daclatasvir have been initiated in several countries. SARS-CoV-2 has an exonuclease-based proofreader to maintain the viral genome integrity. Any effective antiviral targeting the SARS-CoV-2 RdRp must display a certain level of resistance to this proofreading activity. We report here that Sofosbuvir terminated RNA resists removal by the exonuclease to a substantially higher extent than RNA terminated by Remdesivir, another drug being used as a COVID-19 therapeutic. These results offer a molecular basis supporting the current use of Sofosbuvir in combination with other drugs in COVID-19 clinical trials.

SARS-CoV-2, the virus responsible for the COVID-19 pandemic, is a member of the Orthocoronavirinae subfamily<sup>1</sup>. Coronaviruses and hepatitis C virus (HCV) are both positive-sense single-strand RNA viruses<sup>2,3</sup>, with comparable mechanisms requiring an RNA-dependent RNA polymerase (RdRp) for genome replication and transcription. Potential inhibitors have been investigated to target various steps in the Coronavirus infectious cycle, including the viral replication machinery<sup>2</sup>. However, as of now, no effective therapeutic is available to treat serious coronavirus infections such as COVID-19. The RdRp is one of the key targets for antiviral drug development. This RNA polymerase is highly conserved at the amino acid level in the active site among different positive sense RNA viruses, including coronaviruses and HCV<sup>4</sup>. Viral RdRps are highly error-prone<sup>5</sup>, and therefore have the ability to accept modified nucleotide analogues as substrates. Nucleotide and nucleoside analogues that inhibit polymerases comprise an important group of antiviral agents<sup>6-9</sup>.

In late January of 2020, before COVID-19 reached pandemic status, based on our analysis of the molecular structures and activities of hepatitis C viral inhibitors and a comparison of hepatitis C virus and coronavirus replication, we postulated that the FDA-approved hepatitis C drug EPCLUSA (Sofosbuvir/Velpatasvir) might inhibit SARS-CoV-2<sup>10</sup>. Using a computational approach, Elfiky predicted that Sofosbuvir, IDX-184, Ribavirin, and Remdesivir might be potent drugs against COVID-19<sup>11</sup>. We subsequently demonstrated that Sofosbuvir triphosphate is incorporated by the relatively low fidelity SARS-CoV and SARS-CoV-2 RdRps, serving as an immediate polymerase reaction terminator, but not by a host-like high fidelity DNA polymerase<sup>12,13</sup>. We also reported that a library of additional nucleotide analogues with a variety of structural and chemical features terminate RNA

<sup>1</sup>Center for Genome Technology and Biomolecular Engineering, Columbia University, New York, NY 10027, USA. <sup>2</sup>Department of Chemical Engineering, Columbia University, New York, NY 10027, USA. <sup>3</sup>Department of Molecular Pharmacology and Therapeutics, Columbia University, New York, NY 10032, USA. <sup>4</sup>Department of Chemistry, Columbia University, New York, NY 10027, USA. <sup>5</sup>These authors contributed equally: Steffen Jockusch and Chuanjuan Tao. ✉email: dj222@columbia.edu

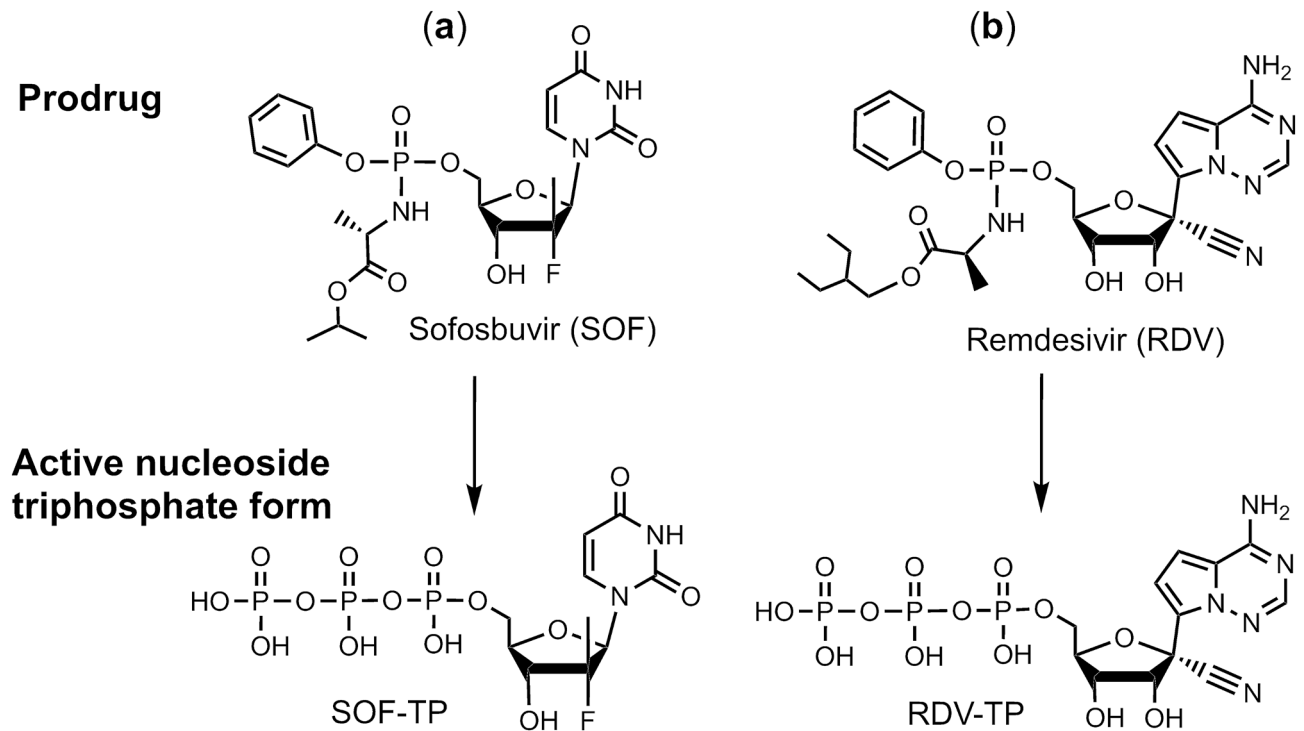


**Figure 1.** Comparison of structures of the prodrugs (a) Sofosbuvir (SOF) and (b) Remdesivir (RDV) and their active triphosphate forms (SOF-TP and RDV-TP). Top: Prodrug (phosphoramidate) forms; Bottom: Active triphosphate forms.

synthesis catalyzed by polymerases of coronaviruses that cause SARS and COVID-19<sup>14</sup>. Gordon et al. performed a kinetic study, including the determination of  $K_m$  values for triphosphates of Remdesivir, Sofosbuvir and other nucleotide analogues<sup>15</sup>. Jácome et al. recently recommended Sofosbuvir as a possible antiviral for COVID-19, based on structural studies and bioinformatic analysis<sup>16</sup>. By comparing the RNA genomes of HCV and SARS-CoV-2, Buonaguro et al. suggested that Sofosbuvir might be an optimal nucleotide analogue to repurpose for COVID-19 treatment<sup>17</sup>. Other investigators have since demonstrated the ability of Sofosbuvir to inhibit SARS-CoV-2 replication in lung and brain cells<sup>18,19</sup>, and COVID-19 clinical trials with EPCLUSA<sup>20</sup> and with Sofosbuvir plus Daclatasvir<sup>21</sup> have been initiated in several countries. Recently, Sadeghi et al. reported encouraging results from a clinical trial using Sofosbuvir (SOF) and Daclatasvir (DCV) as a potential combination treatment for moderate or severe COVID-19 patients<sup>22</sup>. In a study involving 66 patients, these investigators showed that SOF/DCV treatment increased 14-day clinical recovery rates and reduced the length of hospital stays. They indicated that larger well controlled randomized trials are necessary to confirm these results.

Unlike many other RNA viruses, SARS-CoV and SARS-CoV-2 have very large genomes (~30 kb) that encode a 3'-5' exonuclease (nsp14) that carries out proofreading<sup>23,24</sup>; this activity is enhanced by the nsp10 cofactor<sup>25</sup>. This exonuclease-based proofreader increases replication fidelity by removing mismatched nucleotides to maintain the viral genome integrity<sup>26</sup>. Any effective antiviral targeting the SARS-CoV-2 RdRp must display a certain level of resistance to this proofreading activity. Remdesivir (RDV), a nucleotide analogue targeting the SARS-CoV-2 RdRp, is currently used for the treatment of COVID-19 under FDA emergency authorization<sup>27</sup>. The active triphosphate form of Remdesivir possesses a ribose with an OH group at both the 2' and 3' positions, while Sofosbuvir triphosphate has a 2'-F,Me-deoxyribose. The chemical stability of deoxyribose is much higher than that of ribose. Although we and others have demonstrated that Sofosbuvir triphosphate (SOF-TP) can terminate the reaction catalyzed by coronavirus RdRps, it is not known whether Sofosbuvir terminated RNA will offer any resistance to the SARS-CoV-2 exonuclease-based proofreader. We report here that Sofosbuvir terminated RNA resists removal by the exonuclease complex (nsp14/nsp10) to a substantially higher extent than RNA terminated by Remdesivir. We demonstrate for the first time that upon incorporation of the triphosphate form of Sofosbuvir into RNA by the SARS-CoV-2 RdRp, SOF is removed at a lower rate by the SARS-CoV-2 exonuclease complex, relative to RDV and UMP. Thus, not only does the active triphosphate of Sofosbuvir serve as an efficient terminator of the polymerase, but SOF terminated RNA confers a substantial level of resistance to excision by exonuclease. Thus, the current use of Sofosbuvir in combination with other drugs in COVID-19 clinical trials<sup>20,21</sup> is supported by these molecular level results.

## Results

**Comparison of the structure–activity relationships of Sofosbuvir and Remdesivir.** Sofosbuvir (Fig. 1a), a pyrimidine nucleotide analogue prodrug, has a hydrophobic masked phosphate group that enhances its ability to enter host cells. The prodrug is subsequently converted into an active triphosphate form (SOF-TP; 2'-F,Me-UTP) by cellular enzymes, enabling it to inhibit the HCV RdRp NS5B<sup>28,29</sup>. SOF-TP is incorporated into

RNA by the viral RdRp, and due to the presence of fluoro and methyl modifications at the 2' position, inhibits further RNA chain extension, which halts RNA replication and viral multiplication. A related purine nucleotide ProTide<sup>30</sup> prodrug, Remdesivir (Fig. 1b), originally developed for the treatment of Ebola virus infections, though not successfully, is being used for COVID-19 treatment. Unlike Sofosbuvir (Fig. 1a), Remdesivir has both 2'- and 3'-OH groups (Fig. 1b), and a cyano group at the 1' position which is responsible for RdRp inhibition.

Analyzing the structures of the active triphosphate forms of Sofosbuvir (Fig. 1a) and Remdesivir (Fig. 1b), both of which have been shown to inhibit the replication of specific RNA viruses (Sofosbuvir for HCV, Remdesivir for SARS-CoV-2), we noted that the 2'-modifications in Sofosbuvir (the fluoro and methyl groups) are smaller than the 1'-cyano group and the 2'-OH group in Remdesivir. The bulky cyano group in close proximity to the 2'-OH may lead to steric hindrance, thereby impacting the polymerase reaction termination efficiency of the activated form of Remdesivir. It was recently reported that, using the MERS-CoV and SARS-CoV-2 RdRps, RDV-TP had higher incorporation efficiency than ATP<sup>15,31</sup>. However, RDV-TP does not cause immediate polymerase reaction termination; rather, it leads to delayed polymerase termination, likely due to its 1'-cyano group and free 2'-OH and 3'-OH groups.

### SARS-CoV-2 exonuclease resistance study of RNAs terminated by the triphosphates of Sofosbuvir and Remdesivir.

To demonstrate whether the RNA terminated by the triphosphate forms of Sofosbuvir (SOF-TP) and Remdesivir (RDV-TP) have the potential to resist the SARS-CoV-2 proofreading activity, we carried out polymerase extension reactions followed by exonuclease digestion reactions. First, using the replication complex assembled from SARS-CoV-2 nsp12 (the viral RdRp) and nsp7 and nsp8 proteins (RdRp cofactors), the nucleotide analogues were incorporated at the 3' end of the double-stranded segment of the RNA template-loop-primer shown at the top of Fig. 2. Because the template strand consists of an A at the next position, SOF-TP (a UTP analogue) or UTP are incorporated in a single-nucleotide extension reaction. On the other hand, because the next base in the template strand after the A is a U, in order to incorporate the ATP analogue RDV-TP, a two-nucleotide extension (UTP followed by RDV-TP) occurs. After purification to remove the RdRp and nucleoside triphosphates, the extended RNA is treated with the SARS-CoV-2 exonuclease complex consisting of SARS-CoV-2 nsp14 (the viral exonuclease) and nsp10 (an exonuclease cofactor) to determine whether excision of the incorporated nucleotide analogues takes place. Our prediction was that SOF would be at least partially protected from the exonuclease due to the presence of 2'-fluoro and 2'-methyl groups in place of the 2'-OH group, but that RDV and UMP, both of which have a 2'-OH and 3'-OH, would be less protected. This was indeed what we observed as described below.

We performed polymerase extension reactions with SOF-TP, UTP, and RDV-TP + UTP, following the addition of the pre-annealed RNA template-loop-primer to a pre-assembled mixture of nsp12, nsp7 and nsp8. The extended RNA products from the reaction were subjected to MALDI-TOF-MS analysis to confirm that the expected RNA products were formed. The sequence of the RNA template-loop-primer used for the polymerase extension assay, which has previously been described<sup>32</sup>, is shown at the top of Fig. 2.

The MALDI-TOF mass spectrum of the unextended RNA template-loop-primer is shown in Fig. 2a. As shown in Fig. 2b, following incubation with the SARS-CoV-2 replication complex, complete conversion of the RNA template-loop-primer (7851 Da expected) to the Sofosbuvir-terminated extension product was observed (8180 Da observed, 8173 Da expected). Similarly, as shown in Fig. 2c,d, quantitative extension was seen with UTP (8168 Da observed, 8157 Da expected) and by UMP and RDV (8518 Da observed, 8510 Da expected), respectively.

RNA extension products obtained as above were purified and then incubated with the exonuclease complex (nsp14 and nsp10); the results are presented in Fig. 3. The MS trace for the Sofosbuvir extension product (Sofosbuvir-RNA) in the absence of exonuclease (0 min) is shown in Fig. 3a. Only the expected peak at 8183 Da (8173 Da expected) is observed. After 5 min treatment with the nsp14/nsp10 exonuclease complex (Fig. 3b), there is minimal appearance of cleavage products (e.g., the small 6558 Da peak representing cleavage of 5 nucleotides). Even after 30 min exonuclease treatment (Fig. 3c), there is a significant amount of the intact Sofosbuvir-RNA remaining, along with the appearance of lower molecular weight peaks, for example at 6867 Da and 6561 Da (removal of 4 and 5 nucleotides from the 3' end respectively). The MS result for the purified RNA extended with UMP (UMP-RNA) is shown in Fig. 3d (8165 Da observed, 8157 Da expected). In addition to the expected extension peak, a smaller peak at 8472 Da represents mismatch incorporation of an additional U; this is likely due to the high concentration of UTP used and the relatively low fidelity of the RdRp<sup>13</sup>. After 5 min treatment with the exonuclease complex (Fig. 3e), there is substantial cleavage as indicated by the peaks at 7211 Da, 6864 Da and 6559 Da (3, 4 and 5 nucleotide cleavage products, respectively). At 30 min (Fig. 3f), the extended RNA product peak completely disappears with the presence of only cleavage fragment peaks. Finally, for the UMP + RDV extended RNA (Remdesivir-RNA), shown in Fig. 3g, the RNA extension product peak is substantially reduced after 5 min exonuclease treatment (Fig. 3h), with conversion to smaller fragments, e.g., 7210 Da, 6865 Da and 6559 Da (removal of 4, 5 or 6 nucleotides from the 3' end). At 30 min (Fig. 3i), there is no visible Remdesivir-RNA peak remaining, with only cleavage product peaks observed, e.g., at 7209 Da, 6863 Da, 6558 Da and 5923 Da (cleavage of 4, 5, 6 and 8 nucleotides respectively). Clearly, by comparing the results in Fig. 3b with Fig. 3h, and Fig. 3c with Fig. 3i, there is substantially more exonuclease cleavage of Remdesivir-RNA than Sofosbuvir-RNA, and from the results in Fig. 3d–i, it is also apparent that Remdesivir-RNA is cleaved by the SARS-CoV-2 exonuclease more rapidly than RNA extended with UMP.

As a control, exonuclease cleavage results for the unextended RNA template-loop-primer that is used to generate the extended RNA products shown in Fig. 2, are presented in Supplementary Fig. S1. A similar cleavage pattern was observed as in Fig. 3 for natural nucleotide (UMP) or nucleotide analogue (SOF and RDV) extended RNAs. In either case (extended or unextended RNA), the cleavage products with the highest molecular weights

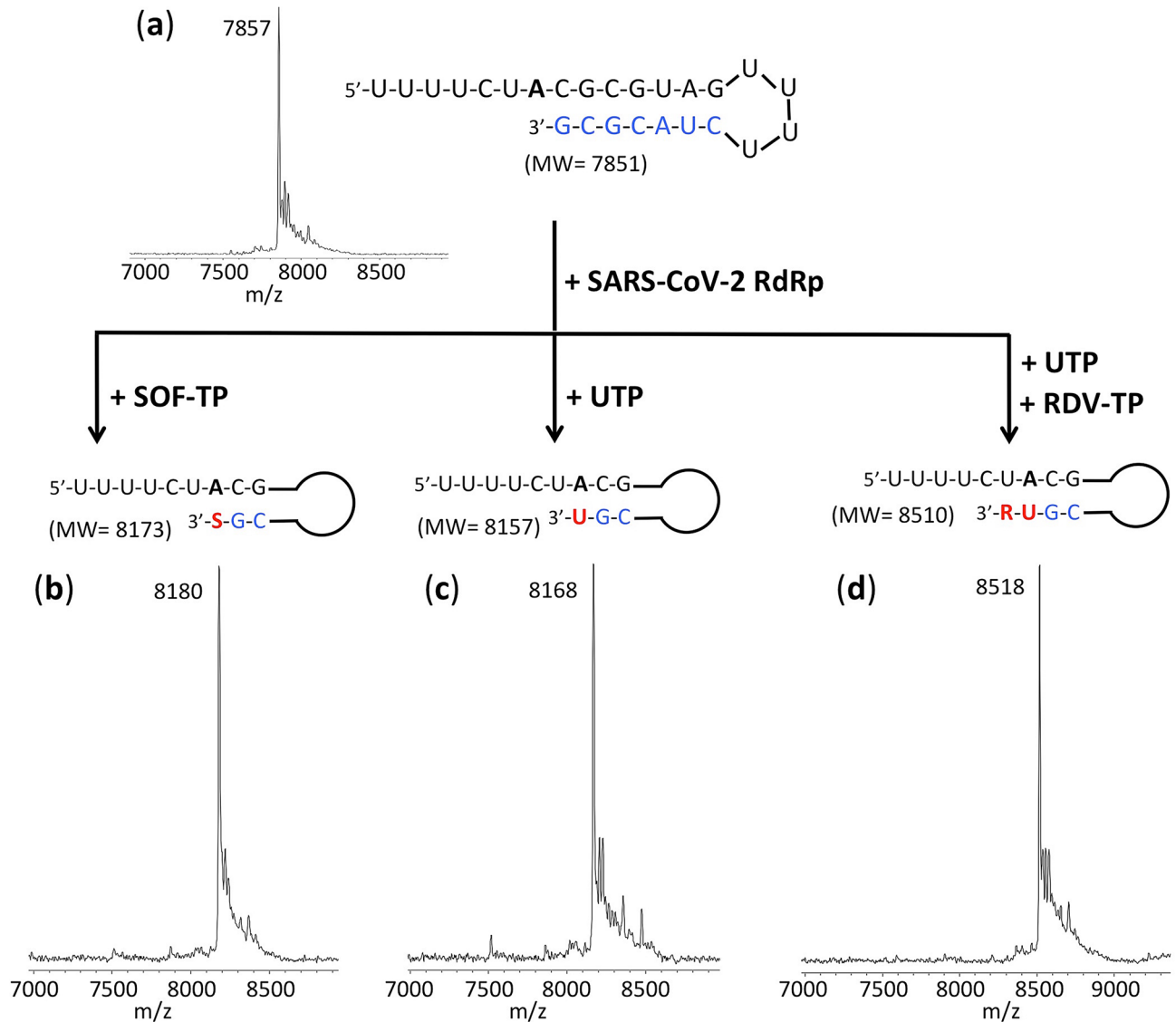


**Figure 2.** Polymerase reactions with SOF-TP, UTP or UTP + RDV-TP to produce RNA extension products. The sequence of the RNA template-loop-primer used for these polymerase extension reactions is shown at the top of the figure. (a) MALDI-TOF mass spectrum of the unextended RNA. Polymerase extension reactions were performed by incubating (b) SOF-TP, (c) UTP and (d) UTP + RDV-TP with pre-assembled SARS-CoV-2 polymerase (nsp12, nsp7 and nsp8) and the indicated RNA template-loop-primer, followed by detection of reaction products by MALDI-TOF MS. The accuracy for  $m/z$  determination is approximately  $\pm 10$  Da.

observed by MALDI-TOF MS indicated removal of 3 or 4 nucleotides. Such rapid cleavage of RNA products by the SARS-CoV exonuclease complex (nsp14/nsp10) has been observed previously<sup>25,26</sup>.

In order to further compare the relative excision among the different extended RNAs, in Fig. 4, similar experiments were carried out as in Fig. 3, but the exonuclease treated SOF and UMP extended RNA products (Fig. 4a,b) were combined for purification, followed by MALDI-TOF-MS analysis. The MS spectrum for the untreated RNA products is shown in Fig. 4a. In the inset it is possible to differentiate the RNA extended with UMP (8163 Da observed, 8157 Da expected) and SOF (8180 Da observed, 8173 Da expected). The MS spectrum for the 15 min exonuclease-treated RNA products is shown in Fig. 4b. It is clear in the inset that the RNA peak representing UMP extension (8164 Da) is reduced to a substantially greater extent than the peak representing the SOF extended RNA (8180 Da). Similarly, the exonuclease treated SOF and UMP + RDV extended RNA products (Fig. 4c–e) were combined for purification, followed by MALDI-TOF-MS analysis. The MS spectrum for the untreated RNA products is shown in Fig. 4c. The peak at 8179 Da represents the SOF extended product and the peak at 8517 Da represents the UMP + RDV extended product. The MS spectrum for the 5 min exonuclease-treated RNA products is shown in Fig. 4d. There is some reduction in the height of the SOF-extended RNA peak, and a much more substantial reduction in the height of the UMP + RDV extended RNA peak. The peaks at 7209 Da, 6864 Da and 6559 Da represent RNA fragments after cleavage of several nucleotides, presumably mainly from the UMP + RDV extended RNA. In the case of the 30 min exonuclease-treated RNA products (Fig. 4e),

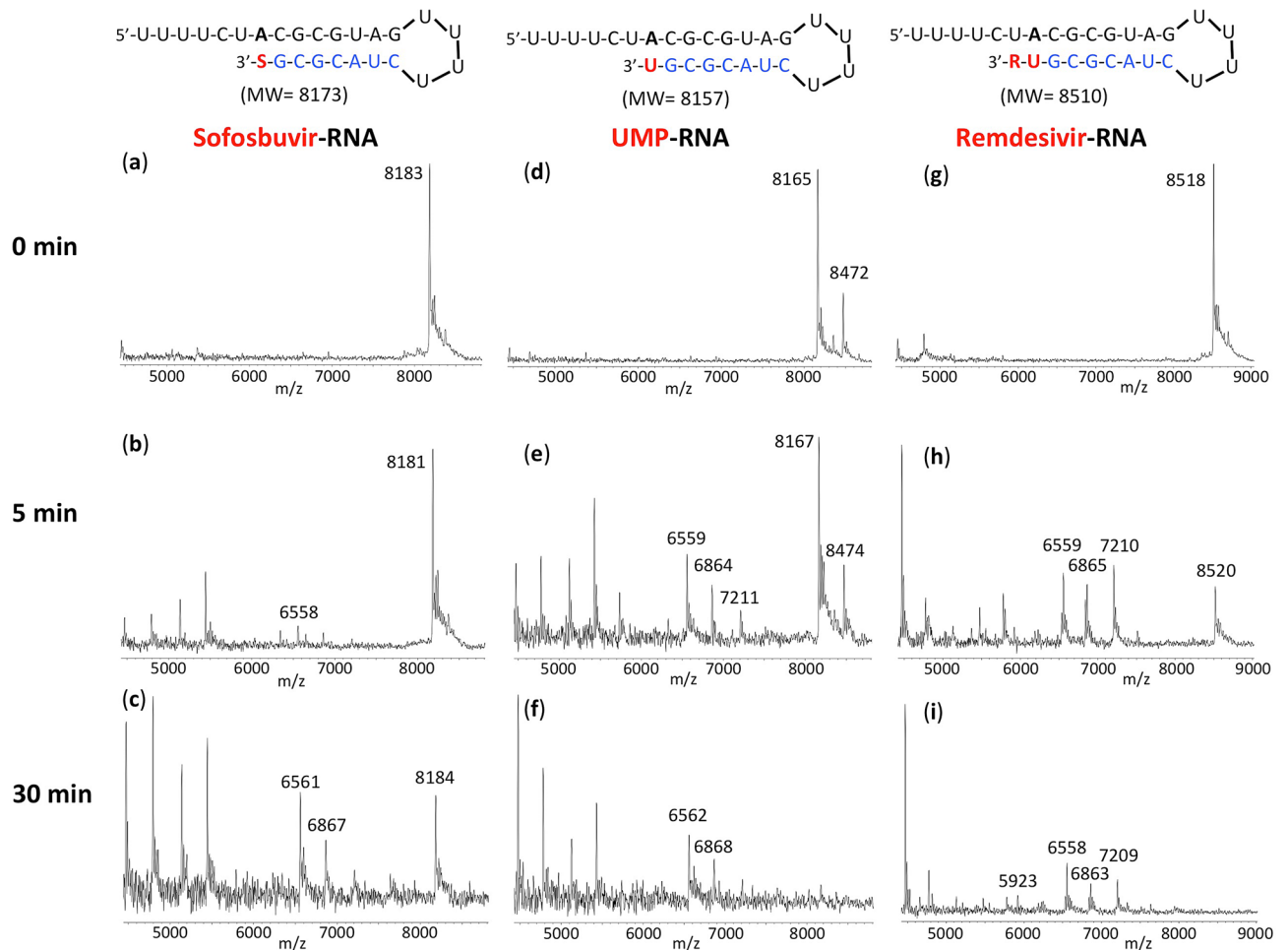


**Figure 3.** Treatment of the RNA products with exonuclease and analysis by MALDI-TOF MS to determine relative excision of Sofosbuvir, UMP and Remdesivir. Untreated products (0 min) are shown in (a) for SOF extended RNA, (d) for UMP extended RNA and (g) for UMP plus RDV extended RNA. Exonuclease reactions were performed by incubating the purified RNA products, generated using the same procedure as in Fig. 2, with pre-assembled SARS-CoV-2 exonuclease complex (nsp14 and nsp10) for 5 min (b,e,h) or 30 min (c,f,i), followed by detection of reaction products by MALDI-TOF MS. The signal intensities were normalized to the highest peak within each time series. The accuracy for m/z determination is approximately  $\pm 10$  Da.

there is still some SOF extended RNA remaining (8183 Da) while the UMP + RDV extended RNA peak is at baseline level. This experiment confirms the results in Fig. 3, that Sofosbuvir is more protected from cleavage by the SARS-CoV-2 exonuclease than UMP or Remdesivir.

## Discussion

Our assay described above, which combines extension of RNA with the nucleotide analogue by the polymerase complex, and subsequent treatment with the exonuclease complex, can be used to test any nucleotide analogues as potential SARS-CoV-2 polymerase inhibitors for their ability to resist exonuclease activity. The template-loop-primers can be designed to allow 1-step extension and termination by nucleotide analogues containing A, C, G or U bases. With MALDI-TOF MS, it is possible to distinguish extension and cleavage of nucleotides differing by  $\sim 10$  Da, especially when included in the same sample as in Fig. 4, a size difference that is not resolvable by assays that utilize gel electrophoresis.

The inhibition of SARS-CoV-2 in cell culture by Sofosbuvir has recently been reported. Sacramento et al. demonstrated that Sofosbuvir inhibited SARS-CoV-2 replication in human hepatoma-derived (Huh-2) and Type II pneumocyte-derived (Calu-3) cells with EC<sub>50</sub> values of 6.2 and 9.5  $\mu$ M, respectively<sup>18</sup>. Mesci et al. showed that Sofosbuvir could protect human brain organoids from SARS-CoV-2 infection<sup>19</sup>. Considering the low toxicity of Sofosbuvir, its ability to be rapidly activated to the triphosphate form by cellular enzymes, and the high intracellular stability of Sofosbuvir triphosphate, Sayad et al. initiated a COVID-19 treatment clinical trial with Sofosbuvir and Velpatasvir, which together form the combination HCV drug EPCLUSA<sup>20</sup>. Izzi et al. also advocated the use of Sofosbuvir and Velpatasvir for the treatment of COVID-19<sup>33</sup>. The Sofosbuvir triphosphate has been shown to persist for over 24 h in hepatocytes<sup>34</sup>. While Remdesivir has been approved under FDA emergency use authorization<sup>27</sup>, and is undergoing safety and efficacy trials for COVID-19, the FDA-approved

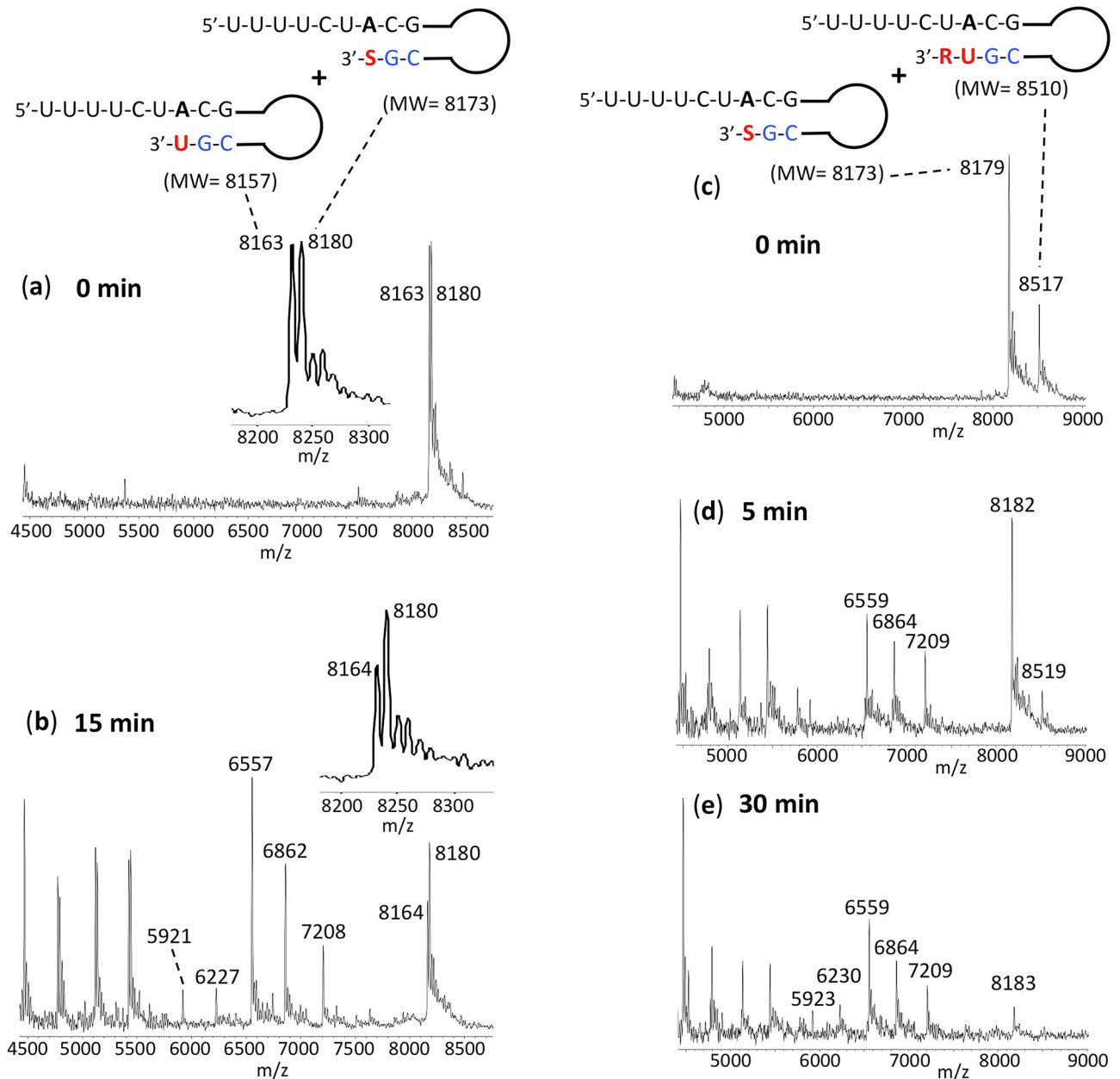


**Figure 4.** Treatment of the RNA products with exonuclease and then combined for analysis by MALDI-TOF MS to determine relative excision of Sofosbuvir, UMP and Remdesivir. Untreated products (0 min) are shown in (a) for SOF and UMP extended RNA and (c) for SOF and UMP + RDV extended RNA. Exonuclease reactions were performed by incubating the purified RNA products with pre-assembled SARS-CoV-2 exonuclease complex (nsp14 and nsp10). The SOF and UMP extended RNAs were treated with the exonuclease complex for 15 min and then combined for purification followed by MALDI-TOF-MS (b). The insets in (a,b) are an enlargement of the 8200–8300 Da portion of the spectrum. The SOF and UMP + RDV extended RNAs were treated with the exonuclease complex for 5 min or 30 min and combined for purification and MALDI-TOF-MS (d,e, respectively). The signal intensities were normalized to the highest peak within each time series. The accuracy for  $m/z$  determination is approximately  $\pm 10$  Da.

hepatitis C drug Sofosbuvir is widely available and has a well-defined safety and clinical profile. Velpatasvir, the other component of EPCLUSA, inhibits NS5A, an essential protein required for HCV replication. NS5A enhances the function of HCV RNA polymerase NS5B during viral RNA genome replication<sup>35,36</sup>. The drug Daclatasvir also inhibits this protein<sup>37</sup>. Daclatasvir was also shown to reduce SARS-CoV-2-induced enhancement of TNF- $\alpha$  and IL-6, key contributors to the cytokine storm, observed in some COVID-19 patients<sup>18</sup>. Because Velpatasvir and Daclatasvir share very similar core structures and target the same NS5A protein in HCV, and Daclatasvir has also been shown to inhibit SARS-CoV-2 replication<sup>18</sup> and is currently in COVID-19 clinical trial<sup>21</sup>, it is plausible that Velpatasvir and other drugs in this class, such as Ledipasvir<sup>38</sup>, Elbasvir<sup>39</sup>, Ombitasvir<sup>40</sup> and Pibrentasvir<sup>41</sup>, will display similar inhibitory activity for SARS-CoV-2.

In summary, we demonstrated that RNA terminated with Sofosbuvir displays substantial resistance to excision by the SARS-CoV-2 exonuclease complex, relative to excision of the natural nucleotide UMP. Moreover, Sofosbuvir appears to show substantially more protection against SARS-CoV-2 exonuclease activity than Remdesivir. These results offer a molecular basis for the use of Sofosbuvir in combination with other drugs in clinical trials for prevention and treatment of COVID-19.

## Methods

The RdRp of SARS-CoV-2, referred to as nsp12, and its two protein cofactors, nsp7 and nsp8, shown to be required for the processive polymerase activity of nsp12, were cloned and purified as described<sup>13</sup>. The 3'-exonuclease, referred to as nsp14, and its protein cofactor, nsp10, were purchased from LSBio (Seattle, WA). Sofosbuvir triphosphate (PSI-7409) was purchased from Sierra Bioresearch (Tucson, AZ). Remdesivir triphosphate (GS-443902) was purchased from MedChemExpress (Monmouth Junction, NJ). UTP was purchased from Fisher Scientific. The RNA oligonucleotide (template-loop-primer) was purchased from Dharmacon (Horizon Discovery, Lafayette, CO).

**Extension reactions with RNA-dependent RNA polymerase.** The RNA template-loop-primer (sequence shown in Fig. 2) was annealed by heating to 75 °C for 3 min and cooling to room temperature in 1 × reaction buffer. The RNA polymerase mixture consisting of 11 μM nsp12, 66 μM nsp8 and 33 μM nsp7 was incubated for 15 min at room temperature in a 1:6:3 ratio in 1 × reaction buffer. Then 10 μL of the annealed RNA template-loop-primer solution (5 μM) in 1 × reaction buffer was added to 9 μL of the RNA polymerase mixture and incubated for an additional 10 min at room temperature. Finally, 1 μL of a solution containing 10 mM SOF-TP (Fig. 2a), 1 mM UTP (Fig. 2b), or 1 mM UTP + 1 mM RDV-TP (Fig. 2c) in 1 × reaction buffer was added and incubation was carried out for 2 h at 30 °C. The final concentrations of reagents in the 20 μL extension reactions were 5 μM nsp12, 30 μM nsp8, 15 μM nsp7, 2.5 μM RNA template-loop-primer, 500 μM SOF-TP (Fig. 2a), 50 μM UTP (Fig. 2b) and 50 μM UTP + 50 μM RDV-TP (Fig. 2c). The 1 × reaction buffer contains the following reagents: 10 mM Tris-HCl pH 8, 10 mM KCl, 2 mM MgCl<sub>2</sub> and 1 mM β-mercaptoethanol. Desalting of the reaction mixture was performed with an Oligo Clean & Concentrator kit (Zymo Research) resulting in ~10 μL purified aqueous RNA solutions. 2 μL of each solution were subjected to MALDI-TOF-MS (Bruker ultrafleXtreme) analysis, following a previously described method<sup>42</sup>. The remaining ~8 μL extended template-loop-primer solutions were used to test exonuclease activity as described below.

**Exonuclease reactions.** The extended RNA template-loop-primers from above (sequences shown in Fig. 3) were annealed by heating to 75 °C for 3 min and cooling to room temperature in 1 × exonuclease reaction buffer. The exonuclease nsp14 (500 nM) and its protein cofactor, nsp10 (2 μM), were incubated for 15 min at room temperature in a 1:4 ratio in 1 × exonuclease reaction buffer. Then 10 μL of the annealed extended RNA template-loop-primer solution (1–1.6 μM) in 1 × exonuclease reaction buffer was added to 10 μL of the exonuclease mixture and incubated at 37 °C for 5, 15 or 30 min. The final concentrations of reagents in the 20 μL reactions were 250 nM nsp14, 1 μM nsp10 and 500–800 nM extended RNA template-loop-primer. The 1 × exonuclease reaction buffer contains the following reagents: 40 mM Tris-HCl pH 8, 1.5 mM MgCl<sub>2</sub>, 50 μM ZnCl<sub>2</sub> and 5 mM DDT. Following desalting using an Oligo Clean & Concentrator (Zymo Research), the samples were subjected to MALDI-TOF-MS (Bruker ultrafleXtreme) analysis. The data shown in Supplementary Fig. S1 for the unextended RNA template-loop-primer is produced in the same way as above.

## Data availability

All relevant data are within the paper.

Received: 14 August 2020; Accepted: 17 September 2020

Published online: 06 October 2020

## References

- Zhu, N. *et al.* A novel coronavirus from patients with pneumonia in China, 2019. *N. Eng. J. Med.* **382**, 727–733 (2020).
- Zumla, A., Chan, J. F. W., Azhar, E. I., Hui, D. S. C. & Yuen, K.-Y. Coronaviruses: drug discovery and therapeutic options. *Nat. Rev. Drug Discov.* **15**, 327–347 (2016).
- Dustin, L. B., Bartolini, B., Capobianchi, M. R. & Pistello, M. Hepatitis C virus: life cycle in cells, infection and host response, and analysis of molecular markers influencing the outcome of infection and response to therapy. *Clin. Microbiol. Infect.* **22**, 826–832 (2016).
- te Velthuis, A. J. W. Common and unique features of viral RNA-dependent polymerases. *Cell Mol. Life Sci.* **71**, 4403–4420 (2014).
- Selisko, B., Papageorgiou, N., Ferron, F. & Canard, B. Structural and functional basis of the fidelity of nucleotide selection by *Flavivirus* RNA-dependent RNA polymerases. *Viruses* **10**, 59 (2018).
- McKenna, C. E. *et al.* Inhibitors of viral nucleic acid polymerases. Pyrophosphate analogues. *ACS Symp. Ser.* **401**, 1–16 (1989).
- Öberg, B. Rational design of polymerase inhibitors as antiviral drugs. *Antiviral Res.* **71**, 90–95 (2006).
- Eltahla, A. A., Luciani, F., White, P. A., Lloyd, A. R. & Bull, R. A. Inhibitors of the hepatitis C virus polymerase; mode of action and resistance. *Viruses* **7**, 5206–5224 (2015).
- De Clercq, E. & Li, G. Approved antiviral drugs over the past 50 years. *Clin. Microbiol. Rev.* **29**, 695–747 (2016).
- Ju, J., Kumar, S., Li, X., Jockusch, S. & Russo, J. J. Nucleotide analogues as inhibitors of viral polymerases. *bioRxiv* <https://doi.org/10.1101/2020.01.30.927574> (2020).
- Elfiky, A. A. Anti-HCV, nucleotide inhibitors, repurposing against COVID-19. *Life Sci.* **248**, 117477 (2020).
- Ju, J. *et al.* Nucleotide analogues as inhibitors of SARS-CoV polymerase. *bioRxiv* <https://doi.org/10.1101/2020.03.12.989186> (2020).
- Chien, M. *et al.* Nucleotide analogues as inhibitors of SARS-CoV-2 polymerase, a key drug target for COVID-19. *J. Proteome Res.* <https://doi.org/10.1021/acs.jproteome.0c00392> (2020).

14. Jockusch, S. *et al.* A library of nucleotide analogues terminate RNA synthesis catalyzed by polymerases of coronaviruses that cause SARS and COVID-19. *Antiviral Res.* **180**, 104857 (2020).
15. Gordon, C. J. *et al.* Remdesivir is a direct-acting antiviral that inhibits RNA-dependent RNA polymerase from severe acute respiratory syndrome coronavirus 2 with high potency. *J. Biol. Chem.* **295**, 6785–6797 (2020).
16. Jácome, R., Campillo-Balderas, J. A., Ponce de León, S., Becerra, A. & Lazcano, A. Sofosbuvir as a potential alternative to treat the SARS-CoV-2 epidemic. *Sci. Rep.* **10**, 9294 (2020).
17. Buonaguro, L., Tagliamonte, M., Tornesello, M. L. & Buonaguro, F. M. SARS-CoV-2 RNA polymerase as target for antiviral therapy. *J. Transl. Med.* **18**, 185 (2020).
18. Sacramento, C. Q. *et al.* The *in vitro* antiviral activity of the anti-hepatitis C virus (HCV) drugs daclatasvir and sofosbuvir against SARS-CoV-2. *bioRxiv* <https://doi.org/10.1101/2020.06.15.153411> (2020).
19. Mesci, P. *et al.* Sofosbuvir protects human brain organoids against SARS-CoV-2. *bioRxiv* <https://doi.org/10.1101/2020.05.30.125856> (2020).
20. Sayad, B., Sobhani, M. & Khodarahmi, R. Sofosbuvir as repurposed antiviral drug against COVID-19: Why were we convinced to evaluate the drug in a registered/approved clinical trial?. *Arch. Med. Res.* **51**, 577–581 (2020).
21. World Hepatitis Alliance press release: Hepatitis C drugs may offer an inexpensive treatment option for COVID-19. <https://www.worldhepatitisalliance.org/latest-news/infohep/3548907/hepatitis-c-drugs-may-offer-inexpensive-treatment-option-covid-19>.
22. Sadeghi, A. *et al.* Sofosbuvir and daclatasvir compared with standard of care in the treatment of patients admitted to hospital with moderate or severe coronavirus infection (COVID-19): a randomized controlled trial. *J. Antimicrob. Chemother.* <https://doi.org/10.1093/jac/dkaa334> (2020).
23. Ma, Y. *et al.* Structural basis and functional analysis of the SARS coronavirus nsp14–nsp10 complex. *Proc. Natl. Acad. Sci. USA* **112**, 9436–9441 (2015).
24. Shannon, A. *et al.* Remdesivir and SARS-CoV-2: Structural requirements at both nsp12 RdRp and nsp14 exonuclease active-sites. *Antivir. Res.* **178**, 104793 (2020).
25. Bouvet, M. *et al.* RNA 3'-end mismatch excision by the severe acute respiratory syndrome coronavirus nonstructural protein nsp10/nsp14 exoribonuclease complex. *Proc. Natl. Acad. Sci. USA* **109**, 9372–9377 (2012).
26. Ferron, F. *et al.* Structural and molecular basis of mismatch correction and ribavirin excision from coronavirus RNA. *Proc. Natl. Acad. Sci. USA* **115**, E162–E171 (2018).
27. Eastman, R. T. *et al.* Remdesivir: A review of its discovery and development leading to emergency use authorization for treatment of COVID-19. *ACS Cent. Sci.* **6**, 672–683 (2020).
28. Kayali, Z. & Schmidt, W. N. Finally sofosbuvir: an oral anti-HCV drug with wide performance capability. *Pharmgenomics Pers. Med.* **7**, 387–398 (2014).
29. Sofia, M. J. *et al.* Discovery of a  $\beta$ -D-2'-Deoxy-2'- $\alpha$ -fluoro-2'- $\beta$ -C-methyluridine nucleotide prodrug (PSI-7977) for the treatment of hepatitis C virus. *J. Med. Chem.* **53**, 7202–7218 (2010).
30. Alanazi, A. S., James, E. & Mehellou, Y. The ProTide prodrug technology: where next?. *ACS Med. Chem. Lett.* **10**, 2–5 (2019).
31. Gordon, C. J., Tchesnokov, E. P., Feng, J. Y., Porter, D. P. & Götte, M. The antiviral compound remdesivir potently inhibits RNA-dependent RNA polymerase from Middle East respiratory syndrome coronavirus. *J. Biol. Chem.* **295**, 4773–4779 (2020).
32. Hillen, H. S. *et al.* Structure of replicating SARS-CoV-2 polymerase. *Nature* **584**, 154–156 (2020).
33. Izzi, A., Messina, V., Rinaldi, L. & Maggi, P. Sofosbuvir/Velpatasvir as a combination with strong potential activity against SARS-CoV2 (COVID-19) infection: how to use direct-acting antivirals as broad-spectrum antiviral agents. *Eur. Rev. Med. Pharmacol. Sci.* **24**, 5193–5194 (2020).
34. German, P., Mathias, A., Brainard, D. & Kearney, B. P. Clinical pharmacokinetics and pharmacodynamics of Ledipasvir/Sofosbuvir, a fixed-dose combination tablet for the treatment of hepatitis C. *Clin. Pharmacokinet.* **55**, 1337–1351 (2016).
35. Gitto, S., Gamal, N. & Andreone, P. NS5A inhibitors for the treatment of hepatitis C infection. *J. Viral Hepatitis* **24**, 180–186 (2017).
36. Quezada, E. M. & Kane, C. M. The hepatitis C virus NS5A stimulates NS5B during *in vitro* RNA synthesis in a template specific manner. *Open Biochem. J.* **3**, 39–48 (2009).
37. Smith, M. A., Regal, R. E. & Mohammad, R. A. Daclatasvir: A NS5A replication complex inhibitor for hepatitis C infection. *Ann. Pharmacother.* **50**, 39–46 (2016).
38. Afdhal, N. *et al.* Ledipasvir and sofosbuvir for untreated HCV genotype 1 infection. *N. Eng. J. Med.* **370**, 1889–1898 (2014).
39. Lawitz, E. *et al.* Efficacy and safety of 12 weeks versus 18 weeks of treatment with grazoprevir (MK-5172) and elbasvir (MK-8742) with or without ribavirin for hepatitis C virus genotype 1 infection in previously untreated patients with cirrhosis and patients with previous null response with or without cirrhosis (C-WORTHY): a randomised, open-label phase 2 trial. *Lancet* **385**, 1075–1086 (2015).
40. Feld, J. J. *et al.* Treatment of HCV with ABT-450/r-ombitasvir and dasabuvir with ribavirin. *N. Eng. J. Med.* **370**, 1594–1603 (2014).
41. Ng, T. I. *et al.* In vitro antiviral activity and resistance profile of the next-generation hepatitis C virus NS5A inhibitor pibrentasvir. *Antimicrob. Agents Chemother.* **61**, e02558–e2616 (2017).
42. Ju, J. *et al.* Four-color DNA sequencing by synthesis using cleavable fluorescent nucleotide reversible terminators. *Proc. Natl. Acad. Sci. USA* **103**, 19635–19640 (2006).

## Acknowledgements

This research is supported by Columbia University, a grant from the Jack Ma Foundation, a generous gift from the Columbia Engineering Member of the Board of Visitors Dr. Bing Zhao, and Fast Grants to J.J. We thank Dr. Robert Kirchoerfer for providing the RdRp (nsp12, nsp7 and nsp8).

## Author contributions

J.J. conceived and directed the project; the approaches and assays were designed and conducted by J.J., S.J., C.T., X.L., M.C., S.K., I.M., Se.K. and J.J.R., and Data were analyzed by all authors. All authors wrote the manuscript.

## Competing interests

The authors declare no competing interests.

## Additional information

**Supplementary information** is available for this paper at <https://doi.org/10.1038/s41598-020-73641-9>.

**Correspondence** and requests for materials should be addressed to J.J.

**Reprints and permissions information** is available at [www.nature.com/reprints](http://www.nature.com/reprints).



**Publisher's note** Springer Nature remains neutral with regard to jurisdictional claims in published maps and institutional affiliations.



**Open Access** This article is licensed under a Creative Commons Attribution 4.0 International License, which permits use, sharing, adaptation, distribution and reproduction in any medium or format, as long as you give appropriate credit to the original author(s) and the source, provide a link to the Creative Commons licence, and indicate if changes were made. The images or other third party material in this article are included in the article's Creative Commons licence, unless indicated otherwise in a credit line to the material. If material is not included in the article's Creative Commons licence and your intended use is not permitted by statutory regulation or exceeds the permitted use, you will need to obtain permission directly from the copyright holder. To view a copy of this licence, visit <http://creativecommons.org/licenses/by/4.0/>.

© The Author(s) 2020